

Structure and Electrochemical Properties of Polyamide and Polyaniline

Shihai Ding,¹ Danming Chao,¹ Min Zhang,² Wanjin Zhang¹

¹Alan G. MacDiarmid Institute, Jilin University, Changchun 130012, People's Republic of China

²College of Chemistry, Northeast Normal University, Changchun 130021, People's Republic of China

Received 11 January 2007; accepted 6 May 2007

DOI 10.1002/app.26707

Published online 3 December 2007 in Wiley InterScience (www.interscience.wiley.com).

ABSTRACT: Electrochemical properties of well-defined molecular structured polyamide with amine-capped aniline pentamer in the main chain and conventional polyaniline were investigated and discussed. CV results suggest that the synthesized polyamide shows a relatively complicated redox process than conventional polyaniline during potential cycling. Differences in ESI characterization revealed that the synthesized polyamide exhibits higher electronic conductivity and lower resistance than the conventional polyaniline. The analysis of molecular

configuration based upon the quantum chemistry calculation reveal that the difference in electrochemical activity and conductivity should be ascribed to the influence of system energy, skeleton conjugation, and the Fermi energy of the bipolaron model in the polymer molecules. © 2007 Wiley Periodicals, Inc. *J Appl Polym Sci* 107: 3408–3412, 2008

Key words: polyaniline; electrochemical properties; molecular configuration

INTRODUCTION

Conducting polymers have been studied extensively because of their potential applications in sensors,¹ electrochromic devices,² and electrochemical supercapacitors³ as well as active electrode materials.⁴ Polyaniline and its derivatives have been considered as promising materials in various applications^{5,6} due to their versatile properties, for example, good environmental stability, ease of processability, high conductivity,^{7–9} swift change in color with applied potential and a simple, and reversible acid/base doping/dedoping properties.¹⁰ In the recent years, copolymers comprising aniline and substituted anilines have received greater attention.^{11–15} These copolymers consist of units of aniline and substituted aniline in their backbone and possess properties different from the respective pristine homopolymers. Because of their differences in structures and physical/chemical properties from conventional polyaniline, to some extent, they could act as excellent materials for applications instead of the conventional polyaniline in some aspects. In our previous works, a

kind of well-defined molecular-structured polyamide with amine-capped aniline pentamer in the main chain has been successfully synthesized through a simple and convenient approach under mild conditions.¹⁶ To further understand this synthesized polyamide material, especially its electroactivity, electrochemical measurement and structural analysis were applied and the comparison with a conventional polyaniline material was also explored.

The electrochemical impedance spectroscopy (EIS) is a powerful tool, providing a lot of information about the electrochemical characteristics of the interest subject.¹⁷ The polymer films have been subjected widely by EIS for obtaining electrochemical information such as electrolyte resistance, charge-transfer resistance, Faradaic capacitance, etc.^{18,19} Because of its generality to distinguish among different electrochemical processes on the basis of different impedance/frequency responses, EIS technique has been frequently applied in experimental studies of various intrinsically conductive polymers, including polyaniline and substituted polyaniline derivatives, deposited as thin films on different electron conductive substrate.²⁰

Correspondence to: W. Zhang (wjzhang@jlu.edu.cn).

Contract grant sponsor: National Natural Science Foundation of China; contract grant numbers: NNSFC-50473007, NNSFC-20674027.

Contract grant sponsor: National Major Project for Fundamental Research of China; contract grant number: G2003CB615604.

EXPERIMENTAL

Materials

Aniline monomer was distilled under reduced pressure. *N*-phenyl-*p*-phenylenediamine (98%, Aldrich), *p*-phenylenediamine (99%, Beijing Chemical Factory),

oxalyl chloride (98%, Shanghai Chemical Factory), triethylamine (99%, Beijing Chemical Factory), hydrochloric acid (37%, Beijing Chemical Factory), ammonium persulfate (APS, 98%, Tianjin Chemical Factory), methanol (99%, Tianjin Chemical Factory), methylene chloride (99.5%, Tianjin Chemical Factory), diethyl ether (99%, Tianjin Chemical Factory), tetrahydrofuran (THF, 99%, Tianjin Chemical Factory), ammonium hydroxide (30%, Changchun Chemical Factory), *N,N'*-dimethylformamide (DMF, 99.5%, Tianjin Chemical Factory), *N,N'*-dimethylacetamide (DMA, 99%, Beijing Chemical Factory), potassium ferricyanide ($K_3Fe(CN)_6$, 98%, Beijing Chemical Factory), potassium hexacyanoferrate (II) trihydrate ($K_4[Fe(CN)_6] \cdot 3H_2O$, 98%, Beijing Chemical Factory), H_2SO_4 (99%, Beijing Chemical Factory), etc. were used as received. The distilled water from a Millipore system ($>18 \text{ M}\Omega \text{ cm}$) was used in all experiments.

Characterization

The electrochemical measurements were performed with a CHI 660 electrochemical workstation (CHI, USA). The electrochemical impedance measurements were carried out on a Solartron 1255B Frequency Response Analyzer. Preparation of polyamide with amine-capped aniline pentamer in the main chain was done as reported earlier.¹⁶

Polyaniline was prepared as follows: 0.465 g aniline (5 mmol) was dissolved in 20-mL 1.0M H_2SO_4 aqueous solution with constant stirring to form a homogeneous solution. Then, another 20-mL 1.0M H_2SO_4 aqueous solution containing of APS (1.14 g, 5 mmol) was added dropwise into aniline/ H_2SO_4 solution under constant stirring. Polymerization was carried out at room temperature for 24 h. Then the precipitate was filtered, washed with methanol and deionized water to remove impurities, and then dried under vacuum at 60°C for 24 h. The resulting product was pulverized into a fine powder to fit for the use of individual measurements.

About 700- μL polymer-saturated DMA solution was cast on a 3-mm glassy-carbon electrode and evaporated DMA before use. Cyclic voltammograms were recorded at room temperature on polyamide and conventional polyaniline modified glassy-carbon electrodes, using an Ag|AgCl (in saturated KCl so-

lution) electrode as the reference electrode. The modified glassy-carbon electrode was put into a 1.0M H_2SO_4 aqueous solution and scanned the potential with a scan rate of 0.01 V s^{-1} .

The DFT B3LYP calculations with standard polarized 3-21G(d) basis set on these systems were carried out.²¹ All the structural models mentioned in this work were optimized first, and then, the electronic properties were calculated based on their optimized configuration. The calculations were performed using the Gaussian 03 program suite.²²

RESULTS AND DISCUSSION

Figure 1 exhibits the molecular structures of the synthesized polyamide and conventional polyaniline. As depicted in illustration (a), the synthesized polyamide polymer is polyamide with amine-capped aniline pentamer in the main chain. $\text{—}\overset{\text{O}}{\parallel}\text{C—}\overset{\text{O}}{\parallel}\text{C—}$ groups were introduced into the polymer skeleton, which is the main difference in the molecular chain conformation from conventional polyaniline [Fig. 1(b)]. Electrochemical properties of polyamide and conventional polyaniline were studied and compared to investigate the influences of polymer molecular structure on their substantial electrochemical behaviors.

Cyclic voltammograms of polyamide and polyaniline are shown in Figure 2. Both the curves of polyamide and polyaniline exhibit multiple and reversible redox processes during the potential cycling in acidic media. Curve (a) is a typical CV characteristic of polyaniline with two pairs of redox peaks. The first oxidation peak appeared at 0.25 V (peak 1) is due to the transformation from leucoemeraldine state to emeraldine state of polyaniline. The corresponding reduction peak appeared at 0.1 V (peak 1'). Whereas the second oxidation peak at 0.57 V (peak 2) is due to the transformation of emeraldine state to pernigraniline state. And the corresponding reduction peak is around 0.5 V (peak 2'). For polyamide, three pairs of redox current peaks at 0.35 V (peak I)/0.3V (peak I'), 0.5 V (peak II)/0.45 V (peak II'), and 0.7 V (peak III)/0.56 V (peak III') can be observed, which were respectively assigned to the transformation of leucoemeraldine/the first emeraldine oxidation state, the first emeraldine/the second emeraldine oxidation state, and the second emeraldine

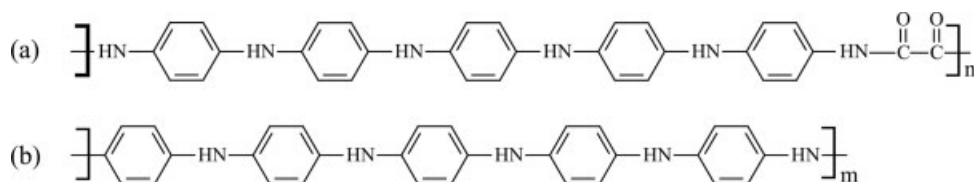


Figure 1 Molecular structures of (a) polyamide and (b) polyaniline.

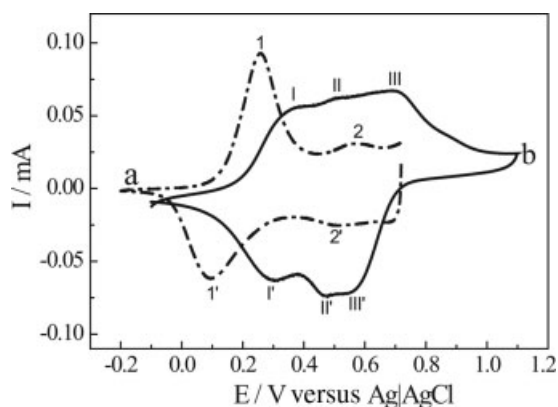


Figure 2 Cyclic voltammograms of the polymer modified carbon-glassy electrode in 1.0M H_2SO_4 supporting electrolyte at 0.01 V s^{-1} versus $\text{Ag}|\text{AgCl}$ reference electrode. (a) polyaniline modified (b) polyamide modified.

dine/pernigraniline oxidation state in molecular chains of polyamide. A more detailed explanation has been described in the early reports.¹⁶ When compared with the conventional polyaniline, the appearance of additional redox peaks in the cyclic voltammograms of polyamide suggests a relatively more complicate electrochemical behavior during the redox process.

When several different scan rates from 0.01 to 1 V were applied during the CV measurements of polyamide modified glassy-carbon electrode, the corresponding curves were obtained and shown in Figure 3. As shown in the inset illustration, both the oxidation and reduction maximum peak current vary as a linear function of the scan rates, which suggests that the oxidation/reduction of polyamide film on the surface of glassy-carbon electrode is an electric charge-transfer controlled process. Moreover,

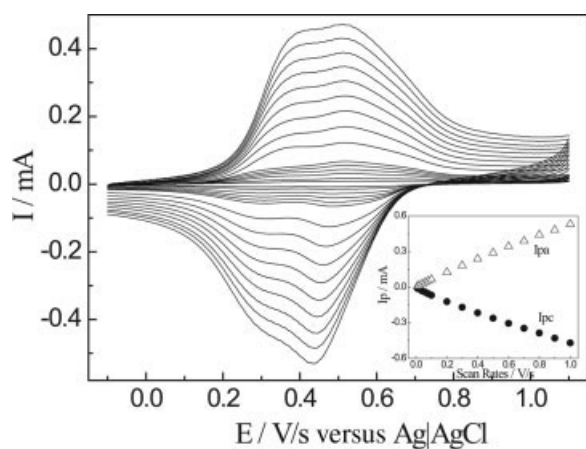


Figure 3 Cyclic voltammograms of polyamide modified glassy-carbon electrode in 1.0M H_2SO_4 scanning at different scan rate from 0.01 to 1 V s^{-1} versus $\text{Ag}|\text{AgCl}$ reference electrode. And inset is calibration plot of maximum peak current versus scan rate.

through the electrochemical integration and calculation, thickness of polyamide film cast on the glassy-carbon electrode is calculated and estimated to be $\sim 180 \text{ nm}$.

The impedance characterization was carried out in a three-electrode electrochemical cuplike cell with a hole at the bottom. The working electrode was a $1.5 \times 2.5 \text{ cm}^2$ Au plate. The Au plate electrode was placed under the bottom hole of the electrochemical cell, where a perfluoroelastomer round ring (1.0 cm in diameter, Kalrez) was inserted to guarantee a sealed equipment as well as definite electrode area. A Pt wire was employed as the counter electrode and all the potentials were measured against an $\text{Ag}|\text{AgCl}$ (in saturated KCl solution) electrode. During the experimental process, DMA solution of polyamide or polyaniline was cast on the round ring area of Au-working electrode and was evaporated to form a thin solid film. Then, 5-mL 2.5 mM $[\text{Fe}(\text{CN})_6]^{3-/4-}$ aqueous solution was added into the electrochemical cell as electrolyte for subsequent ESI measurement.

The EIS curves, as shown in Figure 4, were collected from 0.1 Hz to 100 KHz in 2.5 mM $[\text{Fe}(\text{CN})_6]^{3-/4-}$ aqueous solution at 0.23 mV with an excitation signal of 5 mV. As depicted in Figure 4, the impedance curve of polyamide-modified Au electrodes (curve a) showed a semicircle arc in the high-frequency region and linear spike in the middle and low-frequency region with a slope of 45° . Whereas, EIS of polyaniline (curve b) showed a similar but larger semicircle arc in the high and middle-frequency region and a 45° linear spike in the low-frequency region. As reported, both the curves are in general agreement with typical impedance behavior of polymer film-coated metals in the asymmetric metal/film/electrolyte configuration.²³⁻²⁵ The presence of such semicircle suggests a parallel combination of charge-transfer resistance of reaction and double-layer capacitance at the polymer/electrolyte interface. The straight lines originate from the Warburg diffusion impedance. In spite of the similar

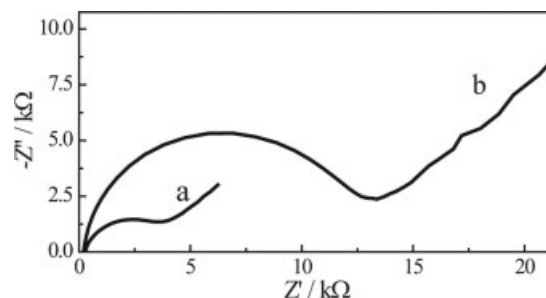


Figure 4 The impedance spectra of (a) polyamide and (b) polyaniline film modified Au electrode in 2.5 mM $[\text{Fe}(\text{CN})_6]^{3-/4-}$ aqueous solution.

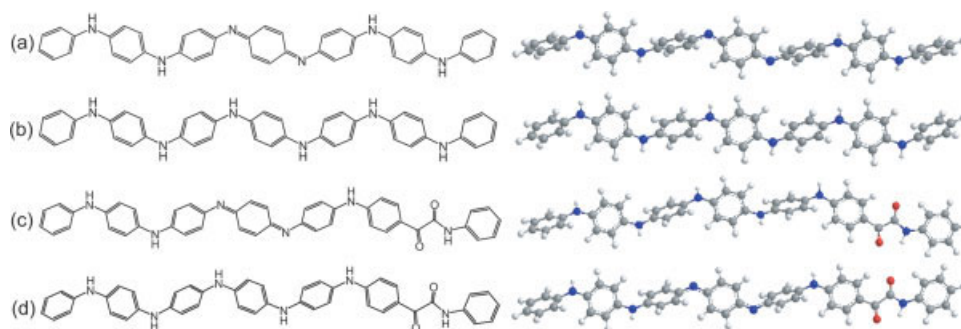


Figure 5 Molecular configuration of oxidized (a) reduced (b) polyaniline repeated segments and oxidized (c) reduced (d) polyamide repeated segments, respectively. [Color figure can be viewed in the online issue, which is available at www.interscience.wiley.com.]

shape of impedance spectra of the two polymers, it clearly shows that there is an obvious difference between the diameters of the two semicircle arcs. The diameter of semicircle of polyamide (curve a) is much smaller than that of polyaniline (curve b), which suggests that the polyamide film presents a lower electrochemical charge transfer resistance than the conventional polyaniline film. In other words, polyamide film exhibits higher electronic conductivity and lower resistance than those of the conventional polyaniline film. It seems that the

$\begin{array}{c} \text{O} \quad \text{O} \\ || \quad || \\ -\text{C}-\text{C}- \end{array}$ groups in the molecular chains have great influence on the charge transfer and resistance of the polymer.

To explain the differences in electrochemical impedance behaviors between polyamide and polyaniline, their monomer derivatives were optimized and simulated using theoretical research. Four systems listed in Figure 5 model the monomers of the polyaniline and polyamide molecules. The two ends of these systems are terminated with phenyl and amino groups so as to simulate the effect of polymers. All the structures are geometrically optimized. The reduction's LUMO energy for system (d) is -1.93 eV, which is much lower than -0.25 eV for system (b).

It indicates that the introduction of $\begin{array}{c} \text{O} \quad \text{O} \\ || \quad || \\ -\text{C}-\text{C}- \end{array}$ segments into the polymer makes the polyamide redox easily. It is known that there exists torsion angles between the adjacent phenyl planes in the polyaniline molecular chain and it is about 38.9° in our calculations. However, in the polyamide molecular, the torsion entirely vanished for the adjacent phenyl planes linked by $\begin{array}{c} \text{O} \quad \text{O} \\ || \quad || \\ -\text{C}-\text{C}- \end{array}$ segments and others are almost kept their original values similarly to those of polyaniline. On the whole, by introducing

$\begin{array}{c} \text{O} \quad \text{O} \\ || \quad || \\ -\text{C}-\text{C}- \end{array}$ segments into the polyaniline chain, it makes a great promotion for the π -conjugated skeleton plane and electron delocalization. On the other hand, it is well known that the conductance of poly-

aniline and its derivatives mainly depends on H^+ transfer due to the polaron in the molecules. The bioxidation of system (b) was optimized, and the calculated $\Delta E_{\text{HOMO-LUMO}}$ is 0.378 and 0.187 eV, respectively. It indicates that the Fermi energy gap for polyamide including bipolaron is much lower than that of polyaniline. So, the impedance of polyamide is less than that of polyaniline.

CONCLUSIONS

The electrochemical properties of polyaniline and synthesized polyamide were investigated and discussed. In summary, from the analysis of the experimental data obtained from CV, EIS, and theoretical calculations, conclusions could be drawn as follows: (i) the appearance of three pairs of redox peaks in CV measurement of polyamide indicates a relatively more complicated redox process compared with conventional polyaniline. Moreover, through electrochemical calculation and analysis, an electric charge-transfer controlled process during redox of polyamide film on the surface of glassy-carbon electrode can be confirmed. (ii) Impedance spectra of synthesized polyamide and conventional polyaniline depict typical model of polymer film-coated metals in the asymmetric metal/film/electrolyte configuration. The difference in diameters of the semicircle impedance arc indicates that polyamide film exhibits higher electronic conductivity and lower resistance than those of the conventional polyaniline. (iii) Through the analysis of theoretical calculations, influences of molecular structures on the impedance of the polymers were discussed including system energy, skeleton conjugation, and the Fermi energy of the bipolaron model. All the theoretical analysis further provides convincing evidences to the impedance results.

References

- Nalwa, H. S. *Handbook of Organic Conductive Molecules and Polymers*, Vol. 4; Wiley: New York, 1997.

2. Bessière, A.; Duhamel, C.; Badot, J. C.; Lucas, V.; Certiat, M. C. *Electrochim Acta* 2004, 49, 2051.
3. Aribizzani, C.; Mastragastino, M.; Paraventi, R. *Adv Mater* 1996, 8, 331.
4. Novak, P.; Muller, K.; Santhanam, K. S. V.; Hass, O. *Chem Rev* 1997, 97, 207.
5. MacDiarmid, A. G.; Chiang, J. C.; Richter, A. F. *Synth Met* 1987, 18, 285.
6. Cao, Y.; Smith, P.; Heeger, A. J. *Synth Met* 1992, 48, 91.
7. Mathew, R. J.; Yang, D. L.; Mattes, B. R. *Macromolecules* 2002, 35, 7575.
8. Wei, Z. X.; Zhang, Z. M.; Wan, M. X. *Langmuir* 2002, 18, 917.
9. Ghosh, P.; Siddhanta, S. K.; Haque, S. R.; Chakrabarti, A. *Synth Met* 2001, 123, 83.
10. Han, D. X.; Chu, Y.; Yang, L. K.; Liu, Y.; Lv, Z. X. *Colloids Surf A* 2005, 259, 193.
11. Yang, C. H.; Wen, T. C. *J Electrochem Soc* 1994, 141, 2624.
12. Yang, C. H.; Wen, T. C. *J Appl Electrochem* 1994, 24, 166.
13. Yang, C. H.; Wen, T. C. *J Electrochem Soc* 1997, 144, 2078.
14. Wen, T. C.; Huang, L. M.; Gopalan, A. *J Electrochem Soc* 2001, 148, D9.
15. Chen, W. C.; Wen, T. C.; Gopalan, A. *J Electrochem Soc* 2001, 148, E427.
16. Chao, D. M.; Lu, X. F.; Chen, J. Y.; Zhao, X. G.; Wang, L. F.; Zhang, W. J.; Wei, Y. *J Polym Sci Part A: Polym Chem* 2006, 44, 477.
17. Darowicki, K.; Kawula, J. *Electrochim Acta* 2004, 49, 4829.
18. Hu, C. C.; Chu, C. H. *J Electroanal Chem* 2001, 503, 105.
19. Csaok, E.; Vieil, E.; Inzelt, G. *J Electroanal Chem* 2000, 482, 168.
20. Radošević, V. H.; Kvastek, K.; Kraljić-Roković, M. *Electrochim Acta* 2006, 51, 3417.
21. Young, D. C.; *Computational Chemistry*; Wiley: New York, 2001.
22. Frisch, M. J.; Trucks, G. W.; Schlegel, H. B.; Scuseria, G. E.; Robb, M. A.; Cheeseman, J. R.; Montgomery, J. A., Jr.; Vreven, T.; Kudin, K. N.; Burant, J. C.; Millam, J. M.; Iyengar, S. S.; Tomasi, J.; Barone, V.; Mennucci, B.; Cossi, M.; Scalmani, G.; Rega, N.; Petersson, G. A.; Nakatsuji, H.; Hada, M.; Ehara, M.; Toyota, K.; Fukuda, R.; Hasegawa, J.; Ishida, M.; Nakajima, T.; Honda, Y.; Kitao, O.; Nakai, H.; Klene, M.; Li, X.; Knox, J. E.; Hratchian, H. P.; Cross, J. B.; Adamo, C.; Jaramillo, J.; Gomperts, R.; Stratmann, R. E.; Yazyev, O.; Austin, A. J.; Cammi, R.; Pomelli, C.; Ochterski, J. W.; Ayala, P. Y.; Morokuma, K.; Voth, G. A.; Salvador, P.; Dannenberg, J. J.; Zakrzewski, V. G.; Dapprich, S.; Daniels, A. D.; Strain, M. C.; Farkas, O.; Malick, D. K.; Rabuck, A. D.; Raghavachari, K.; Foresman, J. B.; Ortiz, J. V.; Cui, Q.; Baboul, A. G.; Clifford, S.; Cioslowski, J.; Stefanov, B. B.; Liu, G.; Liashenko, A.; Piskorz, P.; Komaromi, I.; Martin, R. L.; Fox, D. J.; Keith, T.; Al-Laham, M. A.; Peng, C. Y.; Nanayakkara, A.; Challacombe, M.; Gill, P. M. W.; Johnson, B.; Chen, W.; Wong, M. W.; Gonzalez, C.; Pople, J. A. *Gaussian 03*, Revision C.02 ed.; Gaussian, Inc.: Wallingford, CT, 2004.
23. Vorotyntsev, M. A.; Badiali, L. P.; Inzelt, G. *J Electroanal Chem* 1999, 472, 7.
24. Tarola, A.; Dini, D.; Salatelli, E.; Andreani, F.; Decker, F. *Electrochim Acta* 1999, 44, 4189.
25. Niu, L.; Li, Q. H.; Wei, F. H.; Chen, X.; Wang, H. *J Electroanal Chem* 2003, 544, 121.